System Evaluation of MU-MIMO and Multi-cluster Allocation in LTE-Advanced Uplink

Akihiko Nishio†, Takashi Iwai‡, Atsushi Matsumoto‡, and Daichi Imamura†

†Tokyo R&D Center, Panasonic Corporation

‡Panasonic Mobile Communications R&D Lab. Co., Ltd.

***Abstract*—Multi-user multiple-input and multiple-output (MU-MIMO) is a key technology for enhancing the spectrum efficiency in cellular mobile communication systems. In the Long Term Evolution (LTE) -Advanced, orthogonal cover code (OCC) has been introduced for the uplink demodulation reference signal (DMRS), which provides orthogonality of the DMRS between different user equipment (UEs). This enables different bandwidth allocations for paired UEs of MU-MIMO, which enables flexible frequency selective scheduling and UE pairing. On the other hand, to further enhance the spectrum efficiency in LTE-Advanced, non-contiguous frequency resource allocation based on clustered discrete Fourier transform-spread orthogonal frequency division multiplexing (clustered DFT-S-OFDM), i.e., multi-cluster transmission, is supported. This paper presents frequency and spatial resource allocation for MU-MIMO with multi-cluster transmission, and evaluates the system performance of MU-MIMO in conjunction with multi-cluster transmissions via system level simulations considering the bandwidth allocation restriction for the paired MU-MIMO UE. It is shown that the combination of multi-cluster transmission and MU-MIMO with different bandwidth allocations significantly improve the performance.**

***Index Terms*—Multi-user MIMO, Clustered DFT-S-OFDM, Frequency selective scheduling, Uplink, LTE-Advanced**

I. Introduction

Advanced evolved universal terrestrial radio access (Advanced E-UTRA), also called Long Term Evolution (LTE)-Advanced, has been standardized in the 3rd Generation Partnership Project (3GPP) as a radio interface for IMT-Advanced [1]. Several technology components have been studied to provide higher spectrum efficiency than the LTE system that was standardized as Release 8 LTE (Rel. 8 LTE). In LTE-advanced uplink, multi-cluster transmissions based on clustered discrete Fourier transform-spread orthogonal frequency division multiplexing (clustered DFT-S-OFDM) as well as DFT-S-OFDM adopted in Rel.8 LTE is used as transmission schemes. Multi-cluster transmission allows for flexible frequency selective scheduling, but also causes an increase of peak-to-average power ratio (PAPR). Therefore, by using a proportional fair scheduler with a limited number of clusters depending on the available transmission power of the user equipment (UE), the average cell throughput can be significantly improved while maintaining the cell-edge user throughput [2][3]. Multi user-multiple-input and multiple-output (MU-MIMO) is also an important technique to improve the cell throughput. In Rel. 8 LTE, different reference signal sequences used for demodulation are utilized depending on the transmission bandwidth. For uplink MU-MIMO, a different cyclic shift is assigned for the reference signals of different UEs that are spatially multiplexed. In other words, orthogonality of the reference signal between users can only be kept in case the same transmission bandwidth is allocated for the paired UEs. Therefore, only spatial multiplexing of UEs with the same transmission bandwidth is possible in practice. In LTE-Advanced, the reference signal is additionally orthogonalized by the Walsh code that has been newly introduced as the orthogonal cover code (OCC). Because OCC is independent of the transmission bandwidth, use of the OCC allows spatial multiplexing of UEs with different transmission bandwidths.

Many studies that have investigated uplink MU-MIMO have also addressed frequency selective scheduling [4][5][6]. However, uplink MU-MIMO with multi-cluster transmission has rarely been studied. Furthermore, few papers have considered the restriction of frequency resource allocation for the paired MU-MIMO UEs. Therefore, in this paper, we present a frequency and spatial resource allocation for MU-MIMO with multi-cluster transmission, and evaluate the system performance of MU-MIMO in conjunction with multi-cluster transmission via system level simulations. We consider the bandwidth allocation restriction for the paired MU-MIMO UEs.

The rest of the paper is organized as follows: Section II describes the frequency and spatial resource allocation for LTE-Advanced uplink, section III presents an outline of system level simulations, parameters, and simulation results. Finally, section IV concludes this paper.

II. Frequency and Spatial Resource Allocation in Uplink

The Rel. 8 LTE and LTE-Advanced frameworks provide time/frequency grids. The time/frequency resource allocation unit for user multiplexing and link adaptation is called a resource block (RB = 180 kHz). In Rel. 8 LTE uplink, UEs always transmit on contiguous sets of RBs in a frequency in order to maintain a single carrier property. The LTE-Advanced uplink follows the same RB structure as Rel. 8 LTE. However, to enhance channel-dependent frequency domain scheduling, transmitting on non-contiguous sets of RBs (i.e., multiple clusters) is allowed. The transmitter structure of a clustered DFT-S-OFDM is shown in Fig. 1.

E-mail: †{nishio.akihiko, imamura.daichi}@jp.panasonic.com
‡{iwai.takashi,matsumoto.atsushi-}@ jp.panasonic.com

978-1-4673-0990-5/12/$31.00 ©2012 IEEE

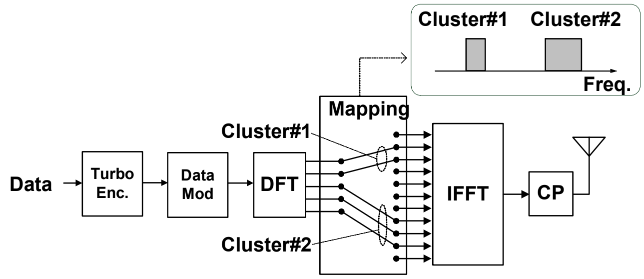

Fig. 1 Transmitter structure of clustered DFT-S-OFDM.

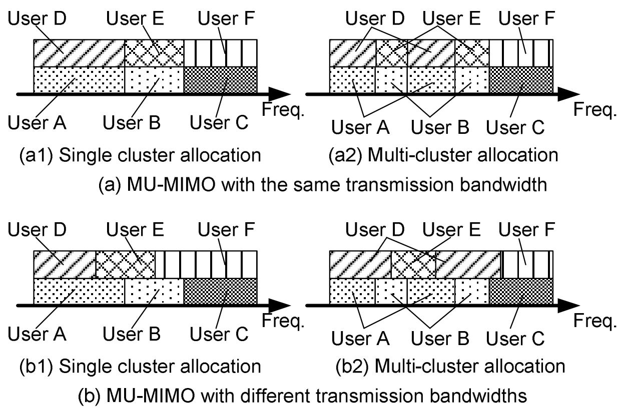

Fig. 2 Frequency resource allocations in MU-MIMO

In addition, spatial resources are allocated in case of MU-MIMO. Fig. 2 shows various frequency resource allocations in MU-MIMO. In LTE, the same transmission bandwidth is allocated to UEs that are spatially multiplexed due to the constraint of the reference signal. Furthermore, only contiguous RB allocation (i.e., single cluster allocation) is allowed. In other words, LTE supports only contiguous RB allocation and the same transmission bandwidth for the paired UEs (Fig. 2(a1)). On the other hand, in LTE-Advanced, in addition to non-contiguous RB allocation (i.e., multi-cluster allocation), it is possible to allocate a different transmission bandwidth for the paired UEs in MU-MIMO (Fig. 2(b1) and (b2)), because of the orthogonality introduced by the OCC on the reference signal. This allows for a flexible frequency and spatial resource allocation, thereby improving the multi-user diversity gain.

The proportional fair (PF)-based scheduling algorithms for MU-MIMO in conjunction with multi-cluster transmission is presented below. We consider the MU-MIMO for UEs with same and different transmission bandwidths.

A. *MU-MIMO with the same transmission bandwidth*

For single cluster allocation and multi-cluster allocation with limited number of clusters, it is important to allocate adjacent RBs for the same UE as long as the channel quality is good in order to achieve a high RB utilization. Therefore, we employed the PF scheduling based on transmission bandwidth expansion [7], and extended it to support MU-MIMO. This achieves a good balance between the average cell throughput and the cell-edge user throughput while maintaining a high RB utilization. The scheduler performs the following steps. In this study, two UEs are multiplexed with MU-MIMO.

1) Calculate the PF priority values for UE_k and RB_n for single user transmission and any combination of the paired UE for MU-MIMO. k denotes the UE number (k = 1, 2, …, K) and n denotes the RB number (n = 1, 2, …N). The priority value for RB n and subframe i for single user transmission is expressed as follows:

$$P_k(n) = r_k(n) / R_k \tag{1}$$

R_k and $r_k(n)$ denote the averaged data rate for UE k and the instantaneous data rate for UE k, respectively, in the case where RB n is assigned. The priority value for MU-MIMO with UE k and UE l is calculated as follows:

$$P_{k,l}(n) = r_{k,l}(n) / R_k \qquad k \neq l \tag{2}$$

where $r_{k,l}(n)$ denotes the instantaneous data rate for UE k in the case where RB n is assigned with spatial multiplexing with UE l.

2) Find the maximum priority value among all UEs (and MU-MIMO UE pairs) and all RBs. For single user transmission, the UE with the maximum priority value is expressed as follows.

$$(k', n') = \underset{k,n}{\arg\max}(P_k(n)) \tag{3}$$

For MU-MIMO, the priority values for both paired UEs are added. The pair of UEs (k'and l') and RB n' are selected according to the following equation.

$$(k', l', n') = \underset{k,l,n}{\arg\max}(P_{k,l}(n) + P_{l,k}(n)) \tag{4}$$

For the final scheduler decision, the priority values for single user transmission and MU-MIMO are compared, and the UE(s) and the RB with the largest priority value are selected.

3) Expand the bandwidth of the allocated UE(s) in step 2, i.e., allocate adjacent RBs, until a) another UE (or UE pair) has a higher priority or b) the transmission power of at least one UE of the allocated UE(s) exceeds the maximum. If an MU-MIMO is selected in step 2, the bandwidth is expanded for both UEs together due to the constraint of the same transmission bandwidth, as illustrated in Fig. 3.

4) Set all of the priority values to zero for the allocated RBs during steps 2 and 3.

5) If the transmission power of the allocated UE reaches the maximum, or if the number of allocated clusters reaches the maximum, stop the RB allocation for the UE, i.e., set the metric value for the UE to zero.

6) Repeat steps 2 to 5 until all RBs are assigned or all UEs have reached the condition for stopping, as mentioned in step 5.

7) Pack the unallocated RBs, i.e., for RBs that were not assigned during the above steps, priority values for UEs (or UE pairs) that are assigned to the nearest adjacent RBs are compared, and allocate the UE (or UE pair) that has the larger priority value.

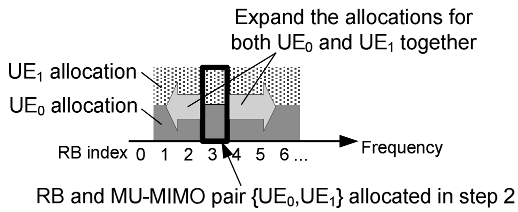

Fig. 3 Bandwidth expansion in step 3 for MU-MIMO with the same transmission bandwidth

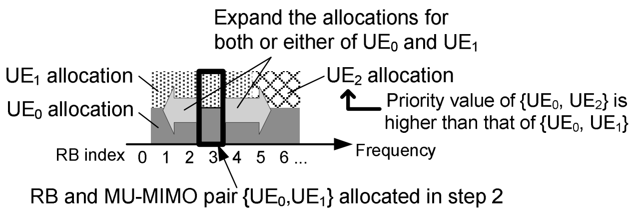

Fig. 4 Bandwidth expansion in step 3 for MU-MIMO with the different transmission bandwidth

B. MU-MIMO with different transmission bandwidth

The scheduling algorithm for MU-MIMO with different transmission bandwidth is similar to the case for MU-MIMO with the same transmission bandwidth, except for the method of expanding the bandwidth, as described in step 3.

The bandwidth expansion procedure in Step 3 is modified as follows. The adjacent RBs are allocated for both or either of the UEs allocated in step 2 until a UE (or UE pair) which is different from both of the allocated UEs has a higher priority, as illustrated in Fig. 4. Here, either of the UEs allocated in step 2 may be replaced with a different UE which has higher priority. For example, in Fig. 4, UE_1 is replaced with UE_2 as the MU-MIMO pair with UE_0 because the priority value of MU-MIMO pair {UE_0, UE_2} is higher than that of {UE_0, UE_1}.

With this algorithm, UE pairs which have higher priority values are allocated during the process of expanding the bandwidth for the allocated UE.

III. Evaluation via System Level Simulation

System level simulations are performed to evaluate multi-cluster transmission and MU-MIMO that have the same and different transmission bandwidths using the above scheduler algorithms. We evaluated both single-cluster and multi-cluster resource allocation with 2 clusters and an unlimited number of clusters. For a comparison, single-input multiple-output (SIMO) is also evaluated.

A. Simulation setup

This subsection provides the simulation methodology and parameters. Simulation assumptions are shown in Table I. The PF scheduler that is outlined in section II is used. A high RB utilization is realized by averaging the PF priority values over 9 RBs for single-cluster allocation and over 3 RBs for multi-cluster allocation.

First, we analyze the power control parameters for both SIMO and MU-MIMO because the power control parameter plays an important role in the uplink system performance. In LTE-Advanced, the setting of the UE transmit power P [dBm] is defined by the following formula [8]

$$P = \min\{ P_{\mathrm{MAX}} , 10 \log_{10}(M) + P_0 + \alpha \cdot PL + \Delta_{\mathrm{TF}} + f \} \quad (5)$$

where min{x, y} denotes the minimum value of x or y. P_{MAX}, M, and PL stand for the maximum transmit power of the UE, the number of RBs allocated to the UE, and the path loss estimate at the UE, respectively. P_0 is a cell-specific parameter and α is a cell-specific path-loss compensation factor of a fractional uplink PC, and both are signaled by a higher layer. Δ_{TF} is the power offset value which is dependent on the channel coding scheme, while f is the accumulated value of PC commands.

The path loss compensation factor α is determined according to the operation policy taking into account the fairness among UEs. In this simulation, $\alpha = 0.8$ is used as a typical operation scenario [4]. The P_0 value is determined considering the balance of the cell throughput and the cell-edge throughput. Fig. 5 and Fig. 6 show the cell throughput and the cell-edge user throughput, which is defined as the fifth percentile of the user throughput for different P_0 values. For cell throughput, a larger P_0 value results in a higher throughput for SIMO because it increases the throughput of cell center users. On the other hand, for MU-MIMO, the cell throughput is reduced from a certain P_0 value because for MU-MIMO, the inter-cell interference level is higher due to doubling of the number of transmitting UEs. Similarly, the cell-edge user throughput has an optimum P_0 value that comes from the trade-off between the allowable transmission power and the inter-cell interference, which is due to the large transmission power.

In this paper, a P_0 value that maximizes the PF utility [9] is employed. The PF utility is a metric that represents a good trade-off between the system throughput and fairness, and is expressed as follows.

$$\text{PF utility} = \frac{1}{N_{user}} \sum_{n=0}^{N_{user}} \log\left(TP_{user\#n}\right) \quad (6)$$

Figure 7 shows the PF utility for SIMO and MU-MIMO. For SIMO and MU-MIMO, the P_0 values that are employed are −84 dBm and −87 dBm, respectively, because they were found to maximize the PF utility. For MU-MIMO, two UEs simultaneously transmit in one cell, so a 3 dB difference for SIMO and MU-MIMO is considered to be reasonable. Using these power control parameters, the cumulative distribution function (CDF) of the IoT (Interference over Thermal noise) is shown in Fig. 8. We observed a similar IoT for SIMO and MU-MIMO.

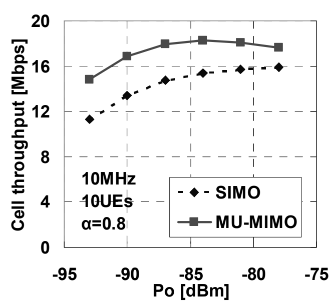

Fig. 5 Cell throughput

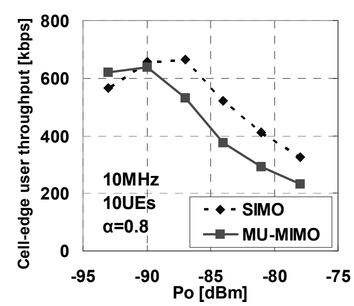

Fig. 6 Cell-edge throughput

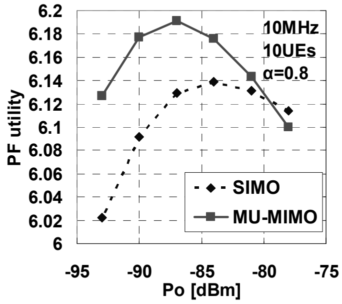

Fig. 7 P0 vs. PF utility

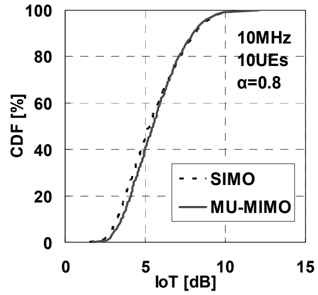

Fig. 8 CDF of IoT

Table I Simulation assumptions

Parameter	Value
System bandwidth	10 MHz (48 RBs)
Carrier frequency	2.0 GHz
Inter-site distance (ISD)	500 m
Number of UEs	5, 10, 15 UEs/cell
Number of clusters	1, 2, Unlimited
Antenna configuration	1 Tx, 4 Rx
UE mobility	3 km/h
Channel model	3GPP Urban Macro (UMa) [10]
Cellular Layout	Hexagonal grid, 19 cell sites, 3 sectors per site
Distance dependent path loss	128.1 + 37.6 log10 (r) [dB] (r: kilometres)
Power control	Refer to Eq. (5)
[P_0, α] for power control	[−84 dBm, 0.8] for SIMO [−87 dBm, 0.8] for MU-MIMO
Maximum transmit power at UE	P_{MAX} = 23dBm for 1cluster 22dBm for 2 clusters 21dBm for >2 clusters [11]
Max. HARQ (re)transmissions	4
Scheduling algorithm	Proportional fairness (PF)
Traffic model	Full buffer
Sounding Reference Signal (SRS) Bandwidth	Adaptive SRS bandwidth (4 / 12 / 24 / 48 RBs)
SRS Feedback period	5 ms
Process delay	6 ms

B. Evaluation of cell throughput and cell-edge user throughput

In this subsection, the average cell throughput and the cell-edge user throughput (which is defined as the fifth percentile user throughput) are evaluated for SIMO and MU-MIMO for UEs with the same transmission bandwidth and with different transmission bandwidths. The following cases are evaluated.

a) Single user transmission (SIMO)
b) MU-MIMO with the same transmission bandwidth
c) MU-MIMO with different transmission bandwidths

For the above cases, single-cluster transmission and multi-cluster transmission (with 2 clusters and with unlimited clusters) are evaluated. Note that even in the case of "MU-MIMO" (i.e., either b) or c)), single user transmission may be selected on a certain RB, depending on the scheduler's decision, as explained in section II.

Figures 7, 8, and 9 show the average cell throughput and the cell-edge user throughput for the above three transmission methods in the case of a 1 × 4 antenna configuration with 5, 10, and 15 UEs per cell, respectively. The value (%) on the bar denotes the gain of the MU-MIMO ((b) and (c)) when compared to that of the SIMO (a).

It is observed that depending on the number of clusters and the number of UEs, MU-MIMO with the same transmission bandwidth improves the cell throughput by 8.8~27% over that of SIMO. The larger gain of MU-MIMO is observed for larger numbers of UEs because the scheduler has more freedom to choose the paired UEs for MU-MIMO. On the other hand, the improvement of the cell-edge user throughput is generally small because of the severe inter-user interference for cell-edge users.

On the other hand, incorporating MU-MIMO with different transmission bandwidths allocation improves both the cell throughput (15.5~42.8% gain) and the cell-edge user throughput (5.9~27.7% gain). In this case, a larger gain is observed for a greater number of clusters. This is because a more flexible selection of paired UEs for MU-MIMO is possible for a larger number of clusters, and is due to the flexible frequency resource allocation. Thus, the combination of multi-cluster transmission and MU-MIMO with different transmission bandwidths can realize a significant improvement in both the cell throughput and the cell-edge user throughput.

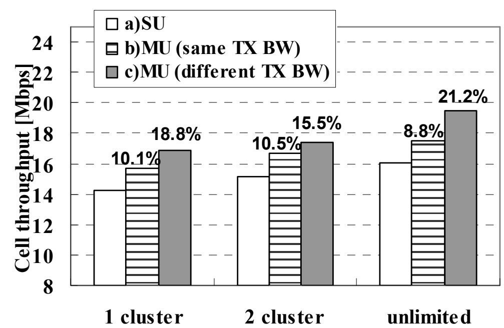

(a) Cell throughput

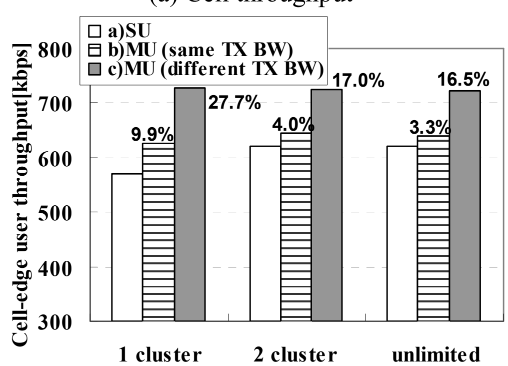

(b) Cell-edge user throughput
Fig. 9 Throughput performance for 5 UEs

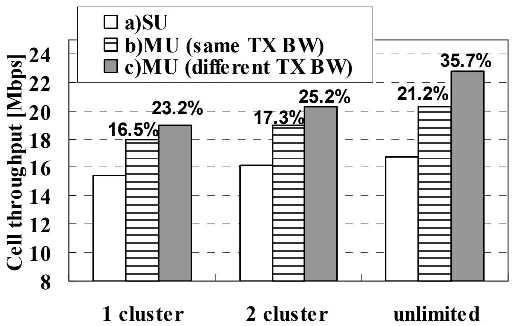

(a) Cell throughput

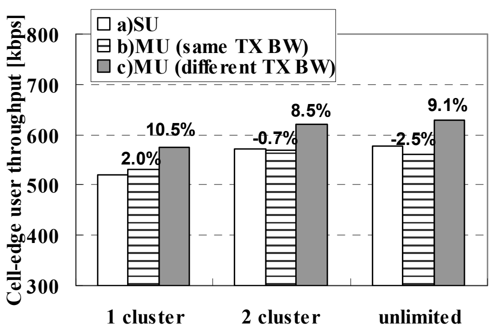

(b) Cell-edge user throughput

Fig. 10 Throughput performance for 10 UEs

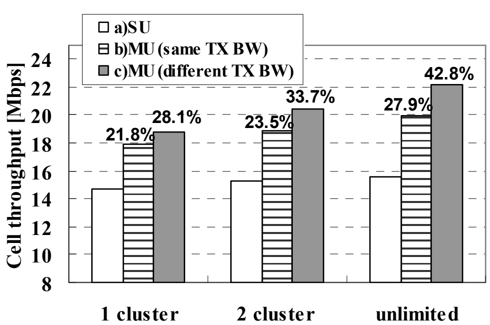

(a) Cell throughput

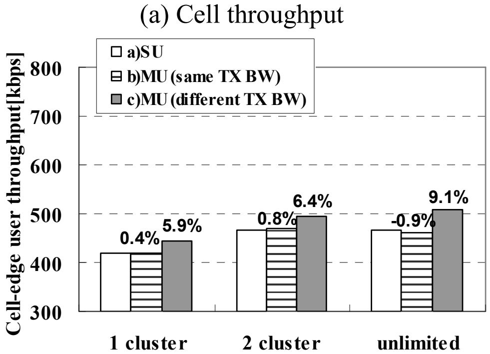

(b) Cell-edge user throughput

Fig. 11 Throughput performance for 15 UEs

IV. CONCLUSIONS

This paper evaluated the performance gain of MU-MIMO compared to the single user transmission (SIMO) in LTE-Advanced uplink with multi-cluster transmission. We considered MU-MIMO both with the same transmission bandwidth and with different transmission bandwidths. The simulation results showed that MU-MIMO with different transmission bandwidths results in improved cell throughput and cell-edge throughput, while MU-MIMO with the same transmission bandwidth contributes mainly to improvements in the cell throughput, especially for a large number of UEs. It was also shown that a combination of multi-cluster transmission and MU-MIMO with different transmission bandwidths led to significant improvements in both the cell throughput and the cell-edge user throughput because it allows for a more flexible UE selection of paired UEs for MU-MIMO.

REFERENCES

[1] 3GPP TS36.300 v10.4.0, "Evolved Universal Terrestrial Radio Access (E-UTRA) and Evolved Universal Terrestrial Radio Access Network (E-UTRAN); Overall Description," June 2011

[2] T.Iwai, A.Matsumoto, S.Takaoka, Y.Ogawa, A.Nishio and D.Imamura "System Performance of Clustered DFT-S-OFDM Considering Maximum Allowable Transmit Power," IEEE International Conference on Communications, 2011

[3] L. Liu, T. Inoue, K. Koyanagi and Y. Kakura, "Uplink Access Schemes for LTE-Advanced," IEICE Trans. Commnun., vol. E92-B, no. 5, pp. 1760-1768, May 2009

[4] D. Nishikawa, T.Kawamura, Y.Kishiyama and T.Nakamura, "Investigation on resource assignment and power control schemes for uplink MU-MIMO in multi-cell environments for LTE/LTE-advanced," 2010 16th Asia-Pacific Conference on Communications(APCC), pp.319-323, Oct. 31 2010-Nov. 3 2010

[5] P.Hosein and T.Wu, "Coordinate ascent scheduler for the multi-user MIMO uplink channel," Personal, Indoor and Mobile Radio Communications, Sept. 2008. PIMRC 2008. IEEE 19th International Symposium on.

[6] H. Lei and X.Li "System level study of LTE uplink employing SC-FDMA and virtual MU-MIMO," Communications Technology and Applications, 2009. ICCTA '09. IEEE International Conference on, pp.152-156, Oct. 16-18 2009

[7] F.D.Calabrese, C.Rosa, M.Anas, P.H.Michaelsen, K.I.Pedersen, P.E.Mogensen, "Adaptive Transmission Bandwidth Based Packet Scheduling for LTE Uplink," Vehicular Technology Conference, 2008. VTC 2008-Fall. IEEE 68th.

[8] 3GPP TS36.213 v 10.2.0, "Evolved Universal Terrestrial Radio Access (E-UTRA); Physical layer procedures," June 2011

[9] F. Kelly, A. Maulloo and D. K. Tan., "Rate control in communication networks: shadow prices, proportional fairness and stability," J. of the Operational Research Society, vol. 49, pp. 237-252, Apr. 1998.

[10] 3GPP TR36.814 v2.0.0, "Technical Specification Group Radio Access Network; Further Advancements for E-UTRA Physical Layer Aspects (Release 9)," March 2010.

[11] 3GPP Document R1-084225, "Comparison between Clustered DFT-s-OFDM and OFDM for supporting non-contiguous RB allocation within a component carrier," November 2008. Available: http://www.3gpp.org.